8-3-2005

Temperature dependence of the training effect in a Co/CoO exchange-bias layer

Christian Binek
University of Nebraska-Lincoln, cbinek@unl.edu

Xi He
University of Nebraska-Lincoln

Srinivas Polisetty
University of Nebraska-Lincoln, polisetty.srinivas@gmail.com

Temperature dependence of the training effect in a Co/CoO exchange-bias layer

Christian Binek, Xi He, and Srinivas Polisetty*
Department of Physics and Astronomy and the Center for Materials Research and Analysis, Ferguson Hall, University of Nebraska, Lincoln, Nebraska 68588-0111, USA

(Received 16 February 2005; revised manuscript received 5 April 2005; published 3 August 2005)

The temperature dependence of the training effect is studied in a Co/CoO exchange-bias bilayer and a phenomenological theory is presented. After field cooling the sample to below its blocking temperature, the absolute value of the exchange-bias field decreases when cycling the heterostructure through consecutive hysteresis loops. This decrease is known as the training effect and is studied in the temperature range $5 \leqslant T \leqslant 120$ K. An implicit sequence, which has been recently derived using the Landau-Khalatnikov approach of relaxation, fits the respective data set for each individual temperature. The underlying discretized dynamic equation involves an expansion of the free energy in powers of the interface magnetization of the antiferromagnetic pinning layer. The particular structure of the free energy with a leading fourth-order term is derived in a mean-field approach. The explicit temperature dependence of the leading expansion coefficient explains the temperature dependence of the training effect. The analytic approach is confirmed by the result of a best fit, which condenses the data from more than 50 measured hysteresis loops.

DOI: 10.1103/PhysRevB.72.054408 PACS number(s): 75.60.−d, 75.70.−i, 75.70.Cn

Nonequilibrium systems provide some of the most challenging problems of modern statistical mechanics.[1,2] Relaxation processes and driven systems represent the major branches of nonequilibrium phenomena. Their complexity becomes apparent when comparing the complete characterization of an equilibrium steady state with its corresponding dynamical problem. The former is determined by the few variables that span the state space while temporal derivatives and gradients are inherent to the full dynamical problem. This paper considers the training of the exchange-bias (EB) effect in the framework of relaxation phenomena. An analytic theory is presented and certain model properties of this nonequilibrium problem of statistical physics are stressed.

EB can take place in magnetic heterostructures where antiferromagnetic (AF) and ferromagnetic (FM) thin films are in close proximity.[3] It is induced by field cooling the heterosystem to below the blocking temperature, T_B, where EB sets in. Usually $T_B < T_N$ holds, where T_N is the Néel temperature of the AF pinning layer. The lateral length scale of the AF order is one of the crucial control parameters of EB.[4–6]

The most striking feature accompanying the EB effect is a shift of the FM hysteresis loop along the magnetic-field axis by the amount $\mu_0 H_{\mathrm{EB}}$. The absolute value of this EB field decreases monotonically when cycling the heterostructure through consecutive hysteresis loops. This training effect is quantified by the $\mu_0 H_{\mathrm{EB}}$ versus n dependence, where n labels the number of loops cycled after initializing the EB via field-cooling. A more appropriate, although not common, term for this gradual degradation of the EB field might be aging instead of training. The strength of this effect depends on the magnetic properties of the AF pinning layer of the heterostructure.[3,7–10] There is a general qualitative consensus that the training effect reflects the deviation of the AF spin structure from its equilibrium configuration. The gradual decrease of $\mu_0 H_{\mathrm{EB}}$ with increasing loop index is a macroscopic fingerprint of configurational rearrangements of the spin structure towards equilibrium. The latter can be literally visualized in the case of Monte Carlo simulations showing the evolution of the AF domain state for consecutively cycled hysteresis loops. Qualitatively similar results have been found for the domain state model where the random field domains of a diluted AF pinning layer carry metastable net interface magnetization[11] and for a defect-free spin-flop model where EB at a compensated interface originates from spin-flop transitions in the grains of a polycrystalline AF pinning layer with randomly oriented uniaxial anisotropies.[12] Moreover, a relaxational approach towards the training effect is supported by the observation of thermally activated temporal relaxation of the EB on laboratory time scales.[13,14]

Recently, based on $T=0$ considerations, Hoffmann pointed out that multiaxial magnetic anisotropy gives rise to a multivalley energy landscape which in turn explains the pronounced training effect between the first and second hysteresis loop of various systems and its absence for uniaxial anisotropic pinning layers.[15] It is a challenging task to find analytic descriptions of the training effect in view of the variety of models which still compete to elucidate the microscopic origin of the stationary exchange-bias effect.[16–20] The recent Stoner-Wohlfarth-type considerations are convincing, but limited to an explanation of $|\mu_0 H_{\mathrm{EB}}(n=1) - \mu_0 H_{\mathrm{EB}}(n=2)| > 0$ or zero in the case of multi- or uniaxial anisotropy. This suggests that a complete description of the training effect is a thermodynamic problem. In addition, the absence of a well established microscopic theory of the EB effect favors a phenomenological approach which is independent of the microscopic details.

A nonstationary EB effect indicates that the spin structure of the AF/FM heterostructure deviates from its equilibrium configuration. Recently, we derived the implicit sequence

$$\mu_0[H_{\mathrm{EB}}(n+1) - H_{\mathrm{EB}}(n)] = -\gamma\{\mu_0[H_{\mathrm{EB}}(n) - H^e_{\mathrm{EB}}]\}^3 \quad (1)$$

from a dicretized Landau-Khalatnikov (LK) equation which describes the relaxation of the AF interface magnetization in an EB heterostructure towards the equilibrium value giving

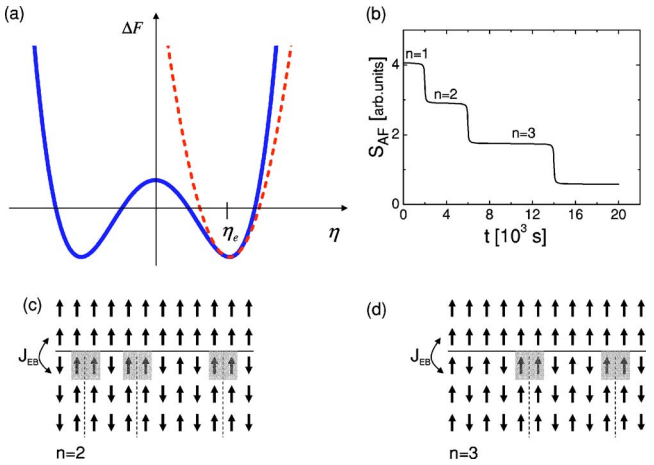

FIG. 1. (Color online) (a) shows a Landau-type free energy (solid line) of the AF pinning layer at $T<T_B$ and the harmonic approximation (dashed line) in the vicinity of η_e. (b) shows a sketch of the temporal evolution of the AF interface magnetization with increasing number n of cycles. (c) and (d) display sketches of the spin structures of the AF/FM bilayer after the second ($n=2$) and third ($n=3$) loop, respectively. Dashed vertical lines indicate AF domain walls. Parallel spin pairs at the interface (horizontal solid line) are highlighted by a gray background. The AF interface magnetization couples with the FM top layer via the exchange J_{EB}.

rise to the equilibrium EB field $\mu_0 H_{EB}^e$.[21] Note that γ is the essential temperature-dependent parameter, which we are going to derive subsequently.

Reference 21 points out that Eq. (1) approaches the empirical but well established $1/\sqrt{n}$ dependence of $\mu_0 H_{EB}$ versus n in the limit $n \gg 1$.[22] Here we sketch an alternative proof of this convergence using a first-order series expansion of $H_{EB}(n+1)$, which becomes a reasonable approximation for $n \gg 1$ with increasing accuracy for increasing n. Substituting the Taylor series into Eq. (1) and integrating the resulting first-order differential equation yields $\mu_0[H_{EB}(n)-H_{EB}^e] = 1/(\sqrt{2\gamma}\sqrt{n})$ for $n \gg 1$. Note that Eq. (1) is more appropriate in describing the training effect than the power law, because the former is derived from a well-founded dynamic equation and allows us to include the description of the first loop at $n=1$. Equation (1) has been successfully applied to the training effect observed in Ref. 23 in NiO/Fe. It represents so far the only analytic approach to the complete description of $\mu_0 H_{EB}$ versus n for $n \geqslant 1$.

Equation (1) originates from the LK first-order differential equation $\xi \dot{S}_{AF} = -\partial \Delta F / \partial S_{AF}$. Here ξ is a phenomenological damping constant, ΔF is the part of the free energy driving the relaxation, and $\dot{S}_{AF}$ is the derivative of S_{AF} with respect to time. The discretization of the equation is realized when $\dot{S}_{AF}$ is replaced by $[S_{AF}(n+1)-S_{AF}(n)]/\tau$, where τ is a characteristic time within the experimental time window of the measurement of the loop. This discretization is in accordance with the experimental fact that the crucial part of the relaxation is triggered by the hysteresis loop of the FM top layer via exchange coupling with the AF pinning layer [see Figs. 1(c) and 1(d)]. In this sense, the discrete nature of the modified LK equation is how the ferromagnet and its coupling J_{EB} with the antiferromagnet enter the theory. There is virtually no relaxation during the time between two successive hysteresis-loop runs since the heterostructure is weakly pinned in a metastable spin configuration.[21] It is this discrete nature of the training effect which makes it unique for the investigation of relaxation phenomena. Experiments on relaxation phenomena deal very often with problematic time scales when typical short spin-flip times or ultraslow spin glass dynamics are involved, for instance. In the case of the training effect, the relaxation process is triggered by the respective hysteresis loop and, hence, the time scale is to a large extent controlled by the experimentalist.

The relation between the AF interface magnetization and the EB field is given by the Meiklejohn-Bean expression according to $\mu_0 H_{EB} = -J_{EB}(S_{AF}S_{FM})/(t_{FM}M_{FM})$, which describes explicitly the dependence of the EB field on a phenomenological coupling J_{EB} between the FM and AF interface magnetization S_{FM} and S_{AF}, respectively, while t_{FM} and M_{FM} are the thickness and the saturation magnetization of the FM layer.[24,25] In the LK approach, the rate of relaxation is determined by the gradient of the free energy with respect to the relaxing parameter. This force drives the system toward equilibrium or a state which corresponds to a pronounced local minimum of the free energy. LK dynamics corresponds to overcritical damping, which is reasonable for the training effect since the relaxation of the interface magnetization is slow in comparison with the microscopic spin fluctuations.[26] Based on the heuristic argument of large spatial spin-spin correlations and, more importantly, the experimental fact that no exponential decay of the EB field is found in the limit $n \gg 1$, we concluded recently that the leading term of a free-energy expansion is of the order $(\delta S_n)^4$, where $\delta S_n = S_{AF}(n) - S_{AF}^e$ and $S_{AF}^e = \lim_{n\to\infty} S_{AF}(n)$ is the AF interface magnetization in the limit of large n. As shown explicitly in Ref. 21, Eq. (1) is a direct result of this structure of the free energy. The parameter γ which enters Eq. (1) is proportional to the leading expansion coefficient of the free energy.[21]

It is the major objective of this paper to derive the free energy and the temperature dependence of its leading expansion coefficient in a mean-field approximation. This result allows us to understand the temperature dependence of the training effect in terms of $\gamma = \gamma(T)$. In the framework of the fluctuation theory of phase transitions, it is a standard approach to expand the free energy with respect to the primary order parameter η in the vicinity of the equilibrium order parameter $\eta_e \neq 0$.[27] This ansatz is in contrast to the usual Landau expansion, which holds close to the critical temperature where $\eta_e \approx 0$. We follow here ideas similar to the fluctuation approach in order to tackle the EB problem because EB takes place at $T<T_B$, where the pinning layer is in its AF phase. The primary order parameter $\eta=(m_1-m_2)/2$ describes the AF order of the pinning layer, while the magnetization $m=(m_1+m_2)/2$ of the AF layer becomes a secondary order parameter. Here, $m_{1,2}$ are the normalized sublattice magnetizations, which are assumed to possess Ising symmetry for simplicity. Eliminating the primary order paramter yields the free energy in terms of m while $\delta S_{AF} \propto m$ links this expansion to the EB effect. At $T<T_N$, the free energy has pronounced minima at $\pm\eta_e$. The field-cooling process selects

one dominant registration of the AF order parameter. Hence it is reasonable to expand the free energy according to

$$\Delta F = \alpha(T)(\eta - \eta_e)^2, \tag{2}$$

where $\alpha(T)$ is a temperature-dependent expansion coefficient. Terms of higher order are neglected. With $\alpha = \tilde{b}\eta_e^2$, Eq. (2) is consistent with the Landau expansion $\Delta F = \tilde{a}\eta^2/2 + \tilde{b}\eta^4/4$ for $T \to T_N$. Figure 1(a) shows the Landau-type free energy of the AF pinning layer below the blocking temperature and the idea of the harmonic approximation in the vicinity of the equilibrium order parameter. In addition, Fig. 1(b) shows a sketch of the evolution of the AF interface magnetization with increasing loop index n. There is virtually no relaxation between two successive hysteresis loops. Relaxation is triggered by the hysteresis loop of the ferromagnet via the coupling with the AF pinning layer. This triggering process gives rise to a steplike decrease of the AF interface magnetization S_{AF}. A microscopic view of the spin structure of the bilayer is presented in Figs. 1(c) and 1(d) after the second ($n=2$) and third ($n=3$) loop, respectively. It points out that AF domains create a magnetic moment m within the layer which in particular contributes to the AF interface magnetization S_{AF}. The latter is reduced by the contribution of one domain wall when comparing the spin structure at $n=3$ with the spin structure at $n=2$. Mean-field theory provides a relation between the primary and secondary order parameters η and m.[28] In zero applied and zero staggered field there is no induced magnetization and, hence, we obtain $m=0$ in equilibrium. The second implicit equation of the self-consistent set of coupled mean-field equations reads[28]

$$\eta = \frac{\sinh\left[\dfrac{2\eta(J+J')}{k_B T}\right]}{\cosh\left[\dfrac{2m(J'-J)}{k_B T}\right] + \cosh\left[\dfrac{2\eta(J+J')}{k_B T}\right]}, \tag{3}$$

where J and J' are related to the number of nearest and next nearest neighbors z and z' and the nearest and next-nearest-neighbor interactions $\tilde{J}$ and $\tilde{J}'$ according to $J = z\tilde{J}$ and $J' = z\tilde{J}'$. $\tilde{J} > 0$ and $\tilde{J}' < 0$ describe AF nearest and next nearest interaction, respectively, while $\tilde{J} < 0$ and $\tilde{J}' > 0$ are FM interactions.

Note that this unusual sign convention of the exchange constants has been introduced by Kincaid and Cohen in order to deal with metamagnetic systems where AF and FM interactions compete.[28,29] In the framework of the mean-field approximation, the critical temperature depends on J and J' according to $T_N = (J+J')/k_B$ while details of the lattice symmetry are neglected. Inspection of Eq. (3) shows that η is an even function of m and, hence, a series expansion of η with respect to m in the vicinity of the equilibrium value $m=0$ reads

$$\eta = \eta(0) + \frac{1}{2}\frac{\partial^2 \eta}{\partial m^2} m^2 + \cdots, \tag{4}$$

where $\eta(0) = \eta_e$. Substitution of the expansion (4) and $\delta S_{\mathrm{AF}} \propto m$ into Eq. (2) yields

$$\Delta F \propto \left[\eta_e \left(\frac{\partial^2 \eta}{\partial m^2}\right)_{m=0}\right]^2 (\delta S_{\mathrm{AF}})^4. \tag{5}$$

The proportionality between δS_{AF} and m takes into account that a residual interface magnetization S_{AF}^e remains in the limit of a large number, n, of cycles and $m \to 0$. The experimental results on Co/CoO, which will be discussed subsequent to the general theoretical considerations, show that the training effect at various constant temperatures $5 < T < 120$ K is successfully fitted by Eq. (1), where γ varies systematically with temperature. The temperature dependence of γ is given in the framework of our above theory by the leading coefficient of the proportionality (5) and reads

$$\gamma(T) \propto \left[\eta_e(T) \left(\frac{\partial^2 \eta(m,T)}{\partial m^2}\right)_{m=0}\right]^2. \tag{6}$$

Hence, an explicit expression $\gamma = \gamma(T)$ requires the calculation of $[\partial^2 \eta(m,T)/\partial m^2]_{m=0}$ and an approximation for $\eta_e(T)$ which holds in a wide temperature range. The second derivative of η with respect to m is calculated via twofold implicit differentiation of Eq. (3). Taking into account that $(\partial \eta/\partial m)_{m=0} = 0$ in accordance with Eq. (4) yields $[\partial^2 \eta(m,T)/\partial m^2]_{m=0}$ as a function of η_e. With this and proportionality (6), one obtains

$$\gamma(\mathrm{T}) = C\left(\frac{\eta_e(T)\tanh\left[\dfrac{T_N\ \eta_e(T)}{T}\right]}{T\left\{T\left(1+\cosh\left[\dfrac{2T_N\ \eta_e(T)}{T}\right]\right) - 2T_N\right\}}\right)^2. \tag{7}$$

Here C becomes a free fitting parameter which summarizes various phenomenological parameters while $\eta_e(T)$ is given by the solution of Eq. (3) for $m=0$. At $T \ll T_N$, where $\eta_e(T) \to 1$, $\eta_e(T) \approx \tanh(T_N/T)$ is the first-order approximation of Eq. (3). In the limit $T \to T_N$, where $\eta_e(T) \to 0$, the equivalent approximation reads $\eta_e(T) \approx (T/T_N)\sqrt{3(T_N - T)/T_N}$, which converges into the Landau-type approximation for $T/T_N \to 1$. Replacing η on the right side of Eq. (3) by the Landau approximation yields

$$\eta_e(T) \approx \tanh\left(\frac{T_N}{T}\sqrt{3(T_N - T)/T_N}\right), \tag{8}$$

which is a useful explicit second-order approximation of $\eta_e(T)$ for all $0 < T \leqslant T_N$. Combining Eqs. (7) and (8) provides an explicit fitting function for the experimental values of γ. Taking into account that the "critical temperature" or more precisely the temperature of vanishing EB is the blocking temperature, T_B, and, hence, replacing T_N by the value $T_B = 186$ K reported in Ref. 30, Eq. (7) becomes a one-parametric fitting function.

The experimental data are obtained from an Al_2O_3/Co/CoO heterostructure, which has been fabricated by dc sputtering of Co on top of the cleaned a plane of a single-crystal plate of Al_2O_3. Before sputtering, the chamber was pumped down to a base pressure of 1.3×10^{-7} mbar. Sputtering took place at an Ar pressure of 6.7×10^{-3} mbar after presputtering the Co target for 10 min. The Co film was deposited at a rate of ≈ 0.2 nm/s for $\Delta t = 500$ s.

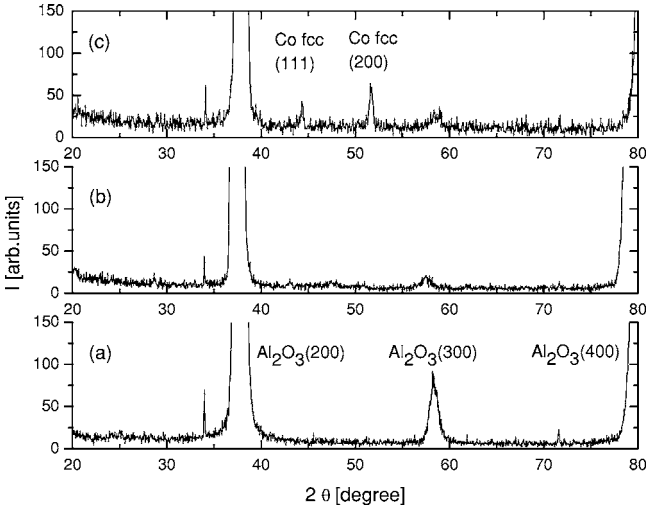

FIG. 2. $\theta-2\theta$ x-ray analysis of the Al_2O_3 substrate (a), the Al_2O_3/Co/CoO heterostructure as prepared (b), and after annealing for 4 h at $T=1000$ K (c). All scans show the dominant (200) and (400) peaks of the single-crystalline Al_2O_3 substrate and its weaker (300) peak. There is no significant additional peak in the as-prepared structure (b). After annealing (c) two additional peaks are observed and assigned as (111) and (200) peaks of fcc Co.

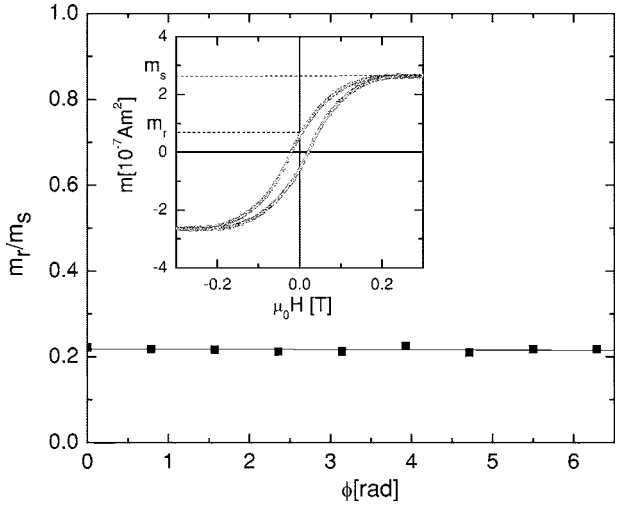

FIG. 3. Ratio m_r/m_S of the remanent and the saturation magnetic moment for various in-plane orientations $0\leqslant\phi\leqslant2\pi$ of the magnetic field. Data are determined from hysteresis loops of Al_2O_3/Co/CoO measured by alternating gradient force magnetometry at room temperature. The inset shows a typical loop. Dashed lines indicate the remanent and the saturation magnetic moment, respectively.

Figure 2 shows the results of the x-ray $\theta-2\theta$ analyis of the substrate (a), and the total heterostructure before (b) and after annealing (c). The latter heat treatment took place under vacuum condition of 2.7×10^{-7} mbar at $T=1000$ K for $\Delta t=4$ h. The x-ray data are obtained with the help of a commercial diffractometer (Rigaku D/Max-B) at Cu K_α radiation with a characteristic wavelenglth of $\lambda\approx0.1544$ nm. Figure 2(a) shows the $\theta-2\theta$ scan of the crystalline Al_2O_3 substrate. The polished surface of the substrate platelet of $d=0.5$ mm thickness corresponds to an a-plane cut in accordance with the strong (h00) reflexes for $h=2$ and 4 and a weaker reflex for $h=3$. Before annealing [Fig. 2(b)], there is no clear signature of the sputtered Co film. However, after annealing [Fig. 2(c)], two additional peaks are observed which are assigned to (111) and (200) peaks of Co in a fcc structure. The latter result can be compared with the structural analysis of epitaxially grown Co on top of the a plane of an Al_2O_3 single crystal.[30] Here, neutron reflectometry shows a pronounced Co fcc (111) peak, but no indication of a (200) peak. This structural difference alters the properties of the magnetic anisotropy. In contrast to the strong planar anisotropy in the epitaxially grown samples of Ref. 30, the sputtered samples show virtually no in-plane anisotropy. The x-ray data in Fig. 2(c) show no signature of a CoO surface layer which, however, reveals its presence in the magnetic data via the EB effect.

Figure 3 shows the ratio m_r/m_s of the remanent magnetic moment m_r and the saturation moment m_s for various angles $0\leqslant\phi\leqslant2\pi$ between the applied planar magnetic field and a fixed direction in the sample plane. Within the uncertainty level of the scatter of the data, there is no systematic variation in m_r/m_s versus ϕ, and, hence, there is no indication for in-plane anisotropy. The solid line represents the best linear fit to the data set and indicates small random scatter around the constant value $m_r/m_s=0.22$. The inset of Fig. 3 shows a typical magnetic hysteresis of the heterostructure measured at room temperature with the help of an alternating gradient force magnetometer. In accordance with the diamagnetic susceptibility of the Al_2O_3 substrate, a linear background has been determined and subtracted for each curve before analyzing the m_r to m_s ratio.

In accordance with the absence of significant anisotropy within the plane, low-temperature hysteresis loops are measured for a fixed but arbitrary direction of the magnetic field in the sample plane. Superconducting quantum interference magnetometry (Quantum Design MPMS XL-7) has been used in order to measure the consecutively cycled magnetic hysteresis loops. Each set of 6–10 consecutive loops is measured after field cooling the sample from $T=320$ K to the target temperatures $T=5$, 25, 50, 65, 75, 80, 105, and 120 K in the presence of an applied planar magnetic field of $\mu_0H=0.3$ T. The strength of this cooling field guaranties saturation of the Co film at a minimal perturbation of the natural AF CoO pinning layer. The training effect at fixed temperature is analyzed with the help of a best fit of Eq. (1). Technical details of the nonlinear fitting procedure of the implicit sequence to the μ_0H_{EB} versus n data are described in Ref. 21.

Figure 4 exemplifies the training effect μ_0H_{EB} versus n for $T=25$ and 75 K (open circles and diamonds, respectively) and the corresponding results of the best fits of Eq. (1) (solid squares and triangles, respectively). The data show the well known enhanced training effect between the first and the second loop as described in Ref. 15, for instance. The two-parametrer fits yield γ and $\mu_0H^e_{EB}$, which in turn are used to calculate the theoretical data from the implicit sequence (1). The inset of Fig. 4 shows $\mu_0H^e_{EB}$ versus T, where $\mu_0H^e_{EB}$ is the extrapolation of $\mu_0H_{EB}(n)$ for $n\rightarrow\infty$. Incidentally, we found a change of the sign of the EB field to posi-

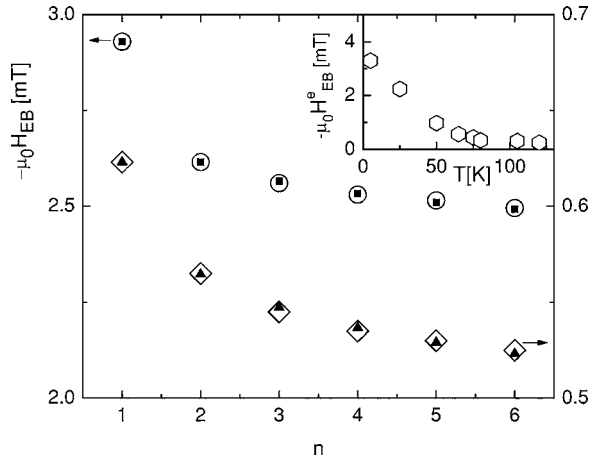

FIG. 4. Training effect $\mu_0 H_{EB}$ versus n for $T=25$ (open circles) and 75 K (diamonds) and the corresponding results of the best fits of Eq. (1) (solid squares and triangles, respectively). Note the different scales for $T=25$ and 75 K, assigned by arrows. Inset shows the equilibrium EB field $\mu_0 H^e_{EB}$ versus T which results from fitting of Eq. (1) to various data sets at $5<T<120$ K.

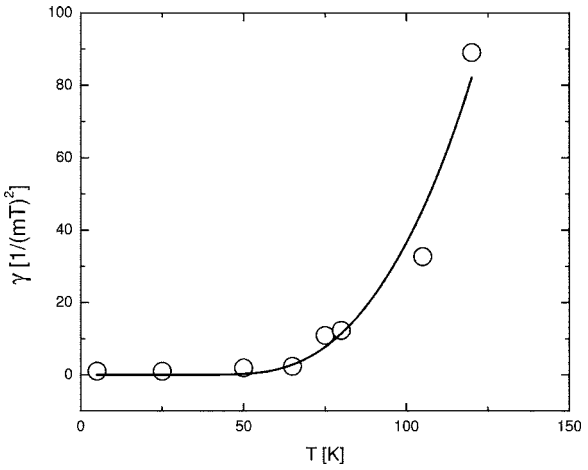

FIG. 5. γ vs T obtained from fitting procedures of Eq. (1) to $\mu_0 H_{EB}$ vs n data for temperatures $5\leqslant T\leqslant 120$ K. The line is a one-parameter best fit of Eq. (7) to γ vs T.

tive values at $T=150$ K very similar to the behavior observed in Ref. 30. However, the tiny absolute value of the EB field did not allow us to perform a reliable analysis of the training effect. It is surprising that we could, however, measure and analyze training effects for absolute values $\mu_0 H_{EB} \gtrsim 0.5$ mT (see Fig. 4, right axis). Here it is crucial to apply the same method of analysis for all hysteresis loops.

A brief description of the procedure of analysis is therefore in order. A linear fit of the magnetization data at $0.51 < \mu_0 H < 0.6$ T of the down branch of the loop has been used to determine the linear background involved in the SQUID measurements. Note that the background is temperature-dependent and has been determined in a separate procedure for each loop. After background subtraction, we determined the coercive fields $\mu_0 H_{c1,2}$ from linear fits, involving data points in a symmetric interval of width $\Delta(\mu_0 H)=30$ mT in the vicinity of the intercepts of the loop with the field axis.

Figure 5 summarizes the results obtained from subsequent fitting procedures of Eq. (1) to all data sets $\mu_0 H_{EB}$ versus n involving more than 50 hysteresis loops. Circles show the resulting γ versus T behavior, which quantifies the temperature dependence of the training effect. The line represents the one parametric best fit of Eq. (7) to the data and is a strong confirmation of the qualitative correctness of the theory outlined above. The resulting fitting parameter reads $C=1.11 \times 10^{12}$ K^4/(mT)^2. Its large value becomes reasonable, when considering $\lim_{T\to T_B} \gamma(T)/C = 9/(16 T_B^4) = 4.7\times 10^{-10}$ K^{-4} for $T_B=186$ K. Note that large values of γ refer to small absolute training effects where the absolute strength of the training effect is quantified according to $\mu_0[H_{EB}(n=\text{const}) - H^e_{EB}]$. This becomes obvious when rearranging Eq. (1) into $\gamma=[\mu_0 H_{EB}(n)-\mu_0 H_{EB}(n+1)]/[\mu_0 H_{EB}(n)-\mu_0 H^e_{EB}]^3$. A large value of γ requires a small denominator, which means small deviations from the equilibrium EB field. In accordance with this tendency, the absolute training effect has to become zero above T_B, where the EB effect is zero for all n. On the other hand, small values of γ correspond to large absolute training effects which are, however, spread over a larger number of cycles. The limiting value $\gamma=0$ at $T=0$ requires a particular discussion. Since $\mu_0 H_{EB}(n)-\mu_0 H^e_{EB}$ remains finite for all n, $\gamma=0$ corresponds to a frozen system where $\mu_0 H_{EB}(n) - \mu_0 H_{EB}(n+1)=0$. Due to the lack of thermal excitations, no change of the EB field is thermally assisted and the system is unable to reach the equilibrium value $\mu_0 H^e_{EB}$ on an experimentally accessible scale of finite n. This tendency of flattening of $\mu_0 H_{EB}$ vs n for decreasing temperature is suggested already in Fig. 4 when comparing the curvature of $\mu_0 H_{EB}$ versus n at $T=75$ and 25 K, respectively.

In summary, a phenomenological theory of the training effect in exchange-bias heterostructures is presented. It provides an analytic description of its thermal evolution. The theory is applied to the training effect in a magnetic Co/CoO heterostructure. Individual training effects are measured by consecutive cycling hysteresis loops at various constant temperatures $5\leqslant T\leqslant 120$ K. The success of the thermodynamic approach is a strong confirmation of a recently derived implicit sequence, which allows us to describe $\mu_0 H_{EB}$ versus n for $n\geqslant 1$ in various systems. It is a future challenging task to find a microscopic theory of the training effect. Even if it turns out that there is no simple unique microscopic theory for the EB effect, training might be a universal property. The predictions made here and in the recent publication[21] allow for further experimental tests. For instance, the relation between the antiferromagnetic interface magnetization and the EB field suggest that γ increases with the square of the ferromagnetic layer thickness and decreases inversely proportional to the square of the ferromagnetic interface magnetization. Both parameters are experimentally accessible.

ACKNOWLEDGMENTS

We would like to express our deep gratitude to Brian Jones and Korey Sorge for supporting the growth, structural, and magnetic characterization of the sample. Further we gratefully acknowledge fruitful discussions with Sitaram Jaswal. This research is supported by NSF-MRSEC.

*Electronic address: cbinek2@unl.edu
†URL: http://www.physics.unl.edu/~cbinek/index.htm

[1] D. Ruelle, J. Stat. Phys. **95**, 393 (1999).
[2] S. Lübeck, Int. J. Mod. Phys. B **18**, 3977 (2004).
[3] J. Nogués and I. K. Schuller, J. Magn. Magn. Mater. **192**, 203 (1999).
[4] Xi Chen, Ch. Binek, A. Hochstrat and W. Kleemann, Phys. Rev. B **65**, 012415 (2001).
[5] Ch. Binek, Xi Chen, A. Hochstrat, and W. Kleemann, J. Magn. Magn. Mater. **240**, 257 (2002).
[6] I. Roshchin, O. Petracic, R. Morales, Li Zhi-Pan, X. Batlle, and I. K. Schuller, e-print cond-mat/0411014.
[7] C. Schlenker, S. S. P. Parkin, J. C. Scott, and K. Howard, J. Magn. Magn. Mater. **54**, 801 (1986).
[8] K. Zhang, T. Zhao, and M. Fujiwara, J. Appl. Phys. **89**, 6910 (2001).
[9] S. G. te Velthuis, A. Berger, and G. P. Felcher, J. Appl. Phys. **87**, 5046 (2001).
[10] W. T. Lee, S. G. E. te Velthuis, G. P. Felcher, F. Klose, T. Gredig, and E. D. Dahlberg, Phys. Rev. B **65**, 224417 (2002).
[11] U. Nowak, K. D. Usadel, J. Keller, P. Miltényi, B. Beschoten, and G. Güntherodt, Phys. Rev. B **66**, 014430 (2002).
[12] D. Suess, M. Kirschner, T. Schrefl, J. Fidler, R. L. Stamps, and J.-V. Kim, Phys. Rev. B **67**, 054419 (2002).
[13] M. D. Stiles and R. D. McMichael, Phys. Rev. B **60**, 12950 (1999).
[14] H. Xi and R. M. White, Phys. Rev. B **64**, 184416 (2001).
[15] A. Hoffmann, Phys. Rev. Lett. **93**, 097203 (2004).
[16] A. P. Malozemoff, Phys. Rev. B **35**, R3679 (1987).
[17] A. E. Berkowitz and Kentaro Takano, J. Magn. Magn. Mater. **200**, 552 (1999).
[18] R. L. Stamps, J. Phys. D **33**, R247 (2000).
[19] P. Miltényi, M. Gierlings, J. Keller, B. Beschoten, G. Güntherodt, U. Nowak, and K. D. Usadel, Phys. Rev. Lett. **84**, 4224 (2000).
[20] M. Kiwi, J. Magn. Magn. Mater. **234**, 584 (2001).
[21] Ch. Binek, Phys. Rev. B **70**, 014421 (2004).
[22] D. Paccard, C. Schlenker, O. Massenet, R. Montmory, and A. Yelon, Phys. Status Solidi **16**, 301 (1966).
[23] A. Hochstrat, Ch. Binek, and W. Kleemann, Phys. Rev. B **66**, 092409 (2002).
[24] W. H. Meiklejohn and C. P. Bean, Phys. Rev. **102**, 1413 (1956).
[25] W. H. Meiklejohn and C. P. Bean, Phys. Rev. **105**, 904 (1956).
[26] G. Vizdrik, S. Ducharme, V. M. Fridkin, and S. G. Yudin, Phys. Rev. B **68**, 094113 (2003).
[27] A. Z. Patashinskii and V. I. Pokrovskii, *Fluctuation Theory of Phase Transitions* (Pergamon, 1979).
[28] J. M. Kincaid and E. G. D. Cohen, Phys. Rep., Phys. Lett. **22**, 57 (1975).
[29] Ch. Binek, *Ising-type Antiferromagnets: Model Systems in Statistical Physics and in the Magnetism of Exchange Bias*, Springer Tracts in Modern Physics Vol. 196 (Springer, Berlin, 2003).
[30] F. Radu, M. Etzkorn, R. Siebrecht, T. Schmitte, K. Westerholt, and H. Zabel, Phys. Rev. B **67**, 134409 (2003).